Supporting Information:

Multifunctional Silicon Optoelectronics Integrated with Plasmonic Scattering Color

Long Wen, Qin Chen*, Xin Hu, Huacun Wang, Lin Jin and Qiang Su

Key Lab of Nanodevices and Applications, Suzhou Institute of Nano-Tech and Nano-Bionics, Chinese Academy of Sciences (CAS), Suzhou 215123, People's Republic of China

*e-mail: qchen2012@sinano.ac.cn

1. Simulation methods for the scattering behavior of the plasmonic nanodiscs.

Three-dimensional FDTD simulations were carried out with the commercial software (Lumerical Solutions), where the scattering problems are solved by implementing the total field/scattered field (TFSF) method. The optical constant of Al was adopted from the Palik's handbook.[1] In our simulations, two open boxes of power monitors surrounding the nanoscatters were used to separately collect the forward and backward portions of the scattering power. The simulation setup is schematically shown in Figure S1.

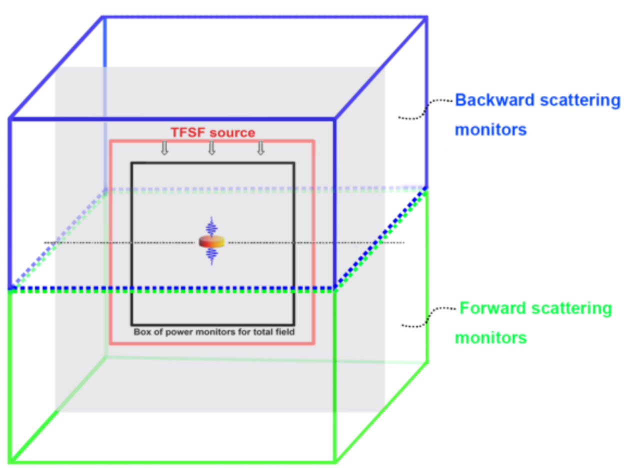

Figure S1. Schematic of the 3D TFSF simulation setup. Two open boxes of power monitors are used to extract the backward and forward portions of the scattering from the nanodiscs.

2. Theoretical calculation of the scattering spectra based on MLWA.

By assuming that the studied nanodiscs can be approximated as oblate spheroid, its static dipolar-polarizability can then be expressed as:[2]

$$\alpha^{\mathrm{static}} = \frac{\varepsilon_{\mathrm{Al}} - \varepsilon_{\mathrm{Eff}}}{\varepsilon_{\mathrm{Eff}} + L(\varepsilon_{\mathrm{Al}} - \varepsilon_{\mathrm{Eff}})} V \tag{S1}$$

here, ε_{Al} and ε_{Eff} are the dielectric functions of bulk Al and the effective surrounding medium. V is the volume of the approximated oblate spheroid and L is a geometrical depolarization factor calculated by the image dipole theory.[3] According to the MLWA, the static polarizability should be modified to account for dynamic depolarization and radiative damping in large nanoparticles. The resulting expression for polarizability is given as follows:

$$\alpha = \alpha^{\mathrm{static}} \left(1 - i\frac{k^3}{6\pi}\alpha^{\mathrm{static}} - \frac{k^2}{2\pi D}\alpha^{\mathrm{static}}\right)^{-1} \tag{S2}$$

where k is the incident wave vector. The scattering efficiency can be therefore written as: $Q_{scat}=k^4|\alpha|^2/(6\pi S)$, where S is the physical cross-section of the nanodiscs. For the homogeneous substrate (n_{Sub}=2) supported nanodiscs, we obtain ε_{Eff}=2.25 by averaging the values of air and the substrate, and L=0.148 for an oblate spheroid with the same dimensions as the nanodiscs (D=120, h=30 nm). Thus, the spectral scattering of a homogeneous substrate supported nanodiscs system can be calculated according to the above equations.

3. Predicted Colors of the plasmonic nanoscatters integrated Si devices.

To evaluate the color tunability of the plasmonic nanoscatters integrated Si devices, the color perceptions relying on CIE 1931 chromaticity diagram were calculated for structures with varied diameters of nanodiscs (D=0 to 200nm). In detail, the XYZ tristimulus values for a color with a spectral reflectance R(λ) were determined using the following formulas:

$$X = k \int_{\lambda 1}^{\lambda 2} \bar{x} R(\lambda) I(\lambda) d\lambda \quad \text{(S3)}$$

$$Y = k \int_{\lambda 1}^{\lambda 2} \bar{y} R(\lambda) I(\lambda) d\lambda \quad \text{(S4)}$$

$$Z = k \int_{\lambda 1}^{\lambda 2} \bar{z} R(\lambda) I(\lambda) d\lambda \quad \text{(S5)}$$

where $\bar{x}$, $\bar{y}$ and $\bar{z}$ are the CIE 1931 color-matching functions, I(λ) is the CIE-D65 illumination and k is a normalization constant. The chromaticity coordinates (*x*, *y*) in CIE 1931 color space are given as:

$$x = \frac{X}{X+Y+Z}, \; y = \frac{Y}{X+Y+Z} \quad \text{(S6)}$$

4. Polarization switchable color images.

The geometric parameters of plasmonic nanoscatters in Figure 6c (marked as pixels 1-4 in main text) are summarized as below:

Parameters	**Pixel 1**	**Pixel 2**	**Pixel 3**	**Pixel 4**
D_x and D_y (nm)	80	76/120	180/116	170/70
P_x and P_y (nm)	230	215/280	330/290	330/210

Table S1. Geometric parameters of the four color pixels in Figure 6c.

The simulated and measured reflection responses of each pixel at x- and y-polarization state are plotted in Figure S2. The results show a very good agreement between the experimental and the theoretical reflectance. This is also generally consistent with the color switching observed in the main text (Figure 6c).

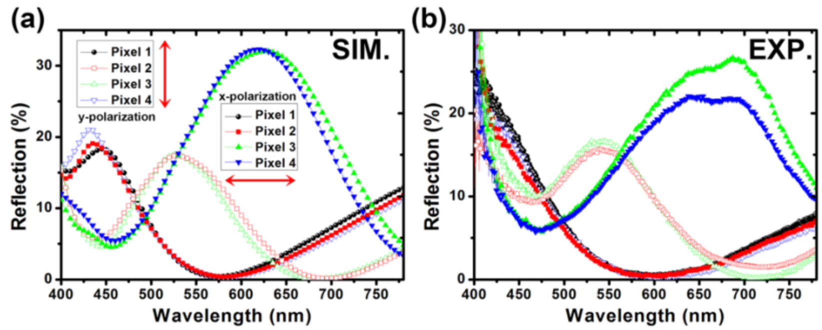

Figure S2. Simulated (a) and measured (b) reflection responses of each pixel at x-polarization (solid) and y-polarization (open) states.

5. IQE of the reference devices.

The measured reflectance and EQE of the reference devices in a wide wavelength regime (300-1100 nm) is depicted in Figure S3. The deduced IQE curve used to calculate the EQE of colored plasmonic devices is also plotted.

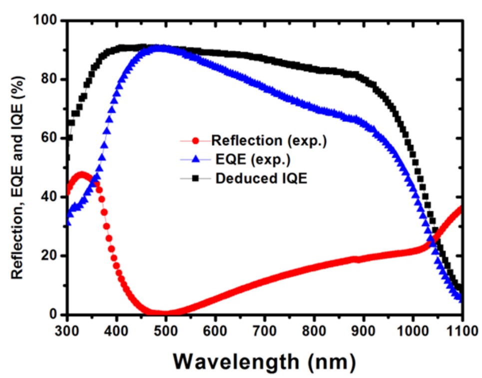

Figure S3. The experimental reflection spectra, EQE and the deduced IQE of the reference device.

6. Photocurrent calculations.

The photocurrent of the devices under one sun illumination can be calculated as:

$$J_{Ph} = e\int_{300}^{1100} \frac{\lambda}{hc} EQE(\lambda)P(\lambda)d\lambda \quad \text{(S7)}$$

where e is the elementary charge, h is Plank's constant, c is the speed of light, P(λ) is AM1.5G spectrum. The resulting photocurrents of the three devices described in main text are found to be 29.39, 29.02 and 28.77 mA/cm^2.

Reference:

1. Smith, D. Y.; Shiles, E.; Inokuti, M. The Optical Properties of Metallic Aluminum. In *Handbook of Optical Constants of Solids*; Palik, E. D., Eds.; Academic Press, Inc.: San Diego, CA, 1997; Vol. 1, pp 369−406.
2. Langhammer, C.; Yuan, Z.; Zoric, I.; Kasemo, B. Plasmonic Properties of Supported Pt and Pd Nanostructures. *Nano Lett.* 2006, 6, 833−838.
3. Fan, X.; Zheng, W.; Singh, D. J. Light Scattering and Surface Plasmons on Small Spherical Particles. *Light: Sci. Appl.* 2014, 3, e179.